

Modelling of graded rectangular micro-plates with variable length scale parameters

Reza Aghazadeh^{1,2a}, Serkan Dag^{*1} and Ender Cigeroglu^{1b}

¹Department of Mechanical Engineering, Middle East Technical University, Ankara 06800, Turkey

²Department of Aeronautical Engineering, University of Turkish Aeronautical Association, Ankara 06790, Turkey

(Received June 2, 2017, Revised January 3, 2018, Accepted January 5, 2018)

Abstract. This article presents strain gradient elasticity-based procedures for static bending, free vibration and buckling analyses of functionally graded rectangular micro-plates. The developed method allows consideration of smooth spatial variations of length scale parameters of strain gradient elasticity. Governing partial differential equations and boundary conditions are derived by following the variational approach and applying Hamilton's principle. Displacement field is expressed in a unified way to produce numerical results in accordance with Kirchhoff, Mindlin, and third order shear deformation theories. All material properties, including the length scale parameters, are assumed to be functions of the plate thickness coordinate in the derivations. Developed equations are solved numerically by means of differential quadrature method. Proposed procedures are verified through comparisons made to the results available in the literature for certain limiting cases. Further numerical results are provided to illustrate the effects of material and geometric parameters on bending, free vibrations, and buckling. The results generated by Kirchhoff and third order shear deformation theories are in very good agreement, whereas Mindlin plate theory slightly overestimates static deflection and underestimates natural frequency. A rise in the length scale parameter ratio, which identifies the degree of spatial variations, leads to a drop in dimensionless maximum deflection, and increases in dimensionless vibration frequency and buckling load. Size effect is shown to play a more significant role as the plate thickness becomes smaller compared to the length scale parameter. Numerical results indicate that consideration of length scale parameter variation is required for accurate modelling of graded rectangular micro-plates.

Keywords: functionally graded micro-plates; strain gradient elasticity; length scale parameters; bending; free vibrations; buckling

1. Introduction

Micro-scale beams and plates are commonly used in micro-electro-mechanical system (MEMS) devices such as micro-sensors, micro-actuators, and micro-resonators. It is experimentally observed that, micro-scale structures exhibit size-dependent mechanical behavior (Andrew and Jonathan 2005, Lam *et al.* 2003, Stölken and Evans 1998). Traditional continuum theories fail to predict the size effect in small-scale structures due to lack of a length scale parameter. Various higher-order continuum theories have been proposed to address the size-dependency. These theories employ one or more intrinsic length scale parameters. Among examples of such theoretical frameworks, we can mention nonlocal elasticity (Eringen 1972), surface elasticity (Gurtin *et al.* 1998), strain gradient theories (Aifantis 1999, Lam *et al.* 2003) and couple stress theories (Mindlin and Tiersten 1962, Toupin 1962, Yang *et al.* 2002). Strain gradient theory (SGT) introduced by Lam

et al. (2003) and modified couple stress theory (MCST) proposed by Yang *et al.* (2002) are the two most commonly used higher order continuum theories in investigations involving small-scale structures. Strain gradient theory is derived by taking into account the second order deformation gradient beside the classical first order deformation gradient, resulting in three material length scale parameters in constitutive relations. Yang *et al.* (2002) incorporated the concept of moment of couples into classical couple stress theory and put forward modified couple stress theory, which employs a single length scale parameter.

Using modified couple stress and strain gradient theories, researchers have developed various models to investigate behavior of homogeneous micro-plates undergoing static bending, free vibrations, or buckling. Akgöz and Civalek (2013), Asghari (2012), Jomehzadeh *et al.* (2011), Tsiatas (2009), Wang *et al.* (2013), Yin *et al.* (2010), Şimşek *et al.* (2015), and Zhong *et al.* (2015) adopted Kirchhoff plate model and analyzed mechanical behavior of homogeneous micro-plates in accordance with modified couple stress theory. In a number of studies, Mindlin plate model, i.e. first order shear deformation theory, and modified couple stress theory is utilized to examine structural mechanics problems of small-scale plates (Ke *et al.* 2012, Ma *et al.* 2011). Farokhi and Ghayesh (2016) used third-order shear deformation theory

*Corresponding author, Professor

E-mail: sdag@metu.edu.tr

^aPh.D.

E-mail: reza.aghazadeh@metu.edu.tr

^bPh.D.

E-mail: ender@metu.edu.tr

in conjunction with modified couple stress theory. Lazopoulos (2009), Ramezani (2012), Wang *et al.* (2011), Akgöz and Civalek (2015), Farokhi and Ghayesh (2015), and Ansari *et al.* (2015) adopted strain gradient theory to capture the size effect in homogeneous micro-plates.

In recent years, incorporation of functionally graded materials (FGMs) into small-scale structures has become feasible with advances in manufacturing technologies such as magnetron sputtering (Fu *et al.* 2003), chemical vapor deposition (Witvrouw and Mehta 2005), and modified soft lithography (Hassanin and Jiang 2014). As a result, structural problems involving functionally graded micro-beams and micro-plates have attracted researchers' attention. Some of these studies are carried out on the basis of modified couple stress theory (Mahmoud and Shaat 2015, Kim and Reddy 2013, 2015, Lou and He 2015, Reddy and Kim 2012, Salehipour *et al.* 2015, Setoodeh and Rezaei 2017, Thai and Choi 2013, Thai and Kim 2013, Thai and Vo 2013). Strain gradient theory is also utilized to examine behavior of functionally graded small-scale structures. Farahmand *et al.* (2015) employed strain gradient theory and Kirchhoff plate model for free vibration analysis of functionally graded micro-plates. In research work conducted by Sahmani and Ansari (2013) and Mohammadimehr *et al.* (2016), strain gradient theory is used in conjunction with third order shear deformation plate model to solve problems regarding FGM micro-plates. Examples of studies based on strain gradient theory and first order shear deformation theory include the articles by Ansari *et al.* (2013), Gholami and Ansari (2016), and Shenias and Malekzadeh (2016).

In all studies mentioned in the foregoing paragraph, length scale parameters of functionally graded micro-plates are assumed to be constants. However, this is a strictly simplifying assumption since the length scale parameter is itself a material property (Mindlin 1963, 1965, Nikolov *et al.* 2007, Park and Gao 2006); and similar to the other material properties of a functionally graded medium it should vary as a function of spatial coordinates. For example, in strain gradient theory, the three length scale parameters are defined in terms of shear modulus and material parameters associated with higher-order deformation measures. Thus, for a functionally graded micro-structure, all of the three length scale parameters are themselves material properties, whose spatial variations need to be represented by suitable functions that depend on the coordinates.

There are several studies in the literature, that account for the spatial variation of the length scale parameter. Kahrobaiyan *et al.* (2012) and Aghazadeh *et al.* (2014) incorporated through-the-thickness variation of the length scale parameter into the analysis of functionally graded micro-beams. Eshraghi *et al.* (2015, 2016) solved problems involving micro-scale FGM annular plates by considering the variation of length scale parameter. Alipour Ghassabi *et al.* (2017) applied nonlocal elasticity to examine free vibrations of rectangular nano-plates having a spatially variable nonlocal parameter. However, in the technical literature, there are no strain gradient theory-based studies that take into account smooth spatial variations of the three

length scale parameters of micro-scale functionally graded rectangular plates. Note that developments presented in Aghazadeh *et al.* (2014) and Kahrobaiyan *et al.* (2012) are applicable for beams, those given in Eshraghi *et al.* (2015, 2016) are valid for annular plates and those described in Alipour Ghassabi *et al.* (2017) are derived in accordance with nonlocal elasticity. Analysis of rectangular FGM micro-plates by means of strain gradient theory requires derivation and solution of completely different partial differential equations compared to those considered in these articles. The main objective in the present study is to put forward *strain gradient theory* based bending, free vibrations and buckling solutions for functionally graded rectangular micro-plates, that possess *spatially variable length scale parameters*.

Governing partial differential equations and associated boundary conditions for bending, free vibrations, and buckling of rectangular FGM micro-plates are derived in accordance with strain gradient theory. All material properties, including the three length scale parameters of strain gradient elasticity, are assumed to be functions of the thickness coordinate in the derivations. Displacement field of the rectangular micro-plate is expressed in a unified way to be able to produce numerical results corresponding to three different plate theories, which are Kirchhoff, Mindlin, and third order shear deformation theories. Equation system comprising partial differential equations and boundary conditions is solved by means of differential quadrature method (DQM). Developed procedures are verified through comparisons made with the results available for limiting cases in the literature. Presented numerical results illustrate influences of length scale parameter variation, and geometric and material parameters upon static deflections, vibration frequencies, and critical buckling loads of functionally graded rectangular micro-plates.

2. Formulation

Fig. 1 depicts a functionally graded rectangular micro-plate having a thickness h . Mid-plane of the undeformed plate is coincident with $x_1 - x_2$ plane. Deformed shape of the mid-plane in $x_1 - x_3$ plane is also shown in Fig. 1. Displacements of any point at time t along x_1, x_2 and x_3 directions are denoted by u_1, u_2 and u_3 , respectively; and can be expressed in a unified form as given below

$$u_1(x_1, x_2, x_3, t) = u(x_1, x_2, t) - x_3 w_{,x_1} + f(x_3) \theta_1(x_1, x_2, t), \quad (1a)$$

$$u_2(x_1, x_2, x_3, t) = v(x_1, x_2, t) - x_3 w_{,x_2} + f(x_3) \theta_2(x_1, x_2, t), \quad (1b)$$

$$u_3(x_1, x_2, x_3, t) = w(x_1, x_2, t), \quad (1c)$$

where u , v and w are displacements of the mid-plane along x_1, x_2 and x_3 , respectively; θ_1 and θ_2 are transverse shear strains of any point on the mid-plane due to

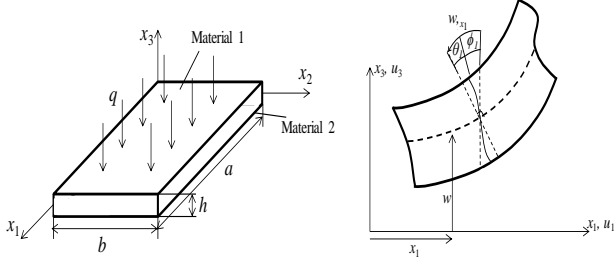


Fig. 1 Configuration and deformed shape of the FGM plate

bending in $x_1 - x_3$ and $x_2 - x_3$ planes; and a comma stands for differentiation. Transverse shear strains θ_1 and θ_2 are written in terms of the mid-plane rotations ϕ_1 and ϕ_2 as follows

$$\theta_1(x_1, x_2, t) = w_{,x_1}(x_1, x_2, t) + \phi_1(x_1, x_2, t), \quad (2a)$$

$$\theta_2(x_1, x_2, t) = w_{,x_2}(x_1, x_2, t) + \phi_2(x_1, x_2, t). \quad (2b)$$

Shape function f in Eq. (1) controls through-the-thickness distributions of transverse shear strain and stress. In the present study, we produce numerical results for three different plate theories, namely Kirchhoff plate theory (KPT), Mindlin plate theory (MPT), and third order shear deformation theory (TSDT). f -functions corresponding to these theories are given by

$$f(x_3) = \begin{cases} 0, & \text{for KPT,} \\ x_3, & \text{for MPT,} \\ x_3 \left(1 - \frac{4x_3^2}{3h^2} \right), & \text{for TSDT.} \end{cases} \quad (3)$$

Note that in Kirchhoff plate theory transverse shear strain is assumed to be zero. Mindlin plate theory presumes constant transverse shear on the cross section. In third order shear deformation theory, transverse shear has a parabolic distribution.

Partial differential equations of motion and boundary conditions are derived by using Hamilton's principle, which postulates that

$$\delta \int_{t_1}^{t_2} (K - (U - W)) dt = 0, \quad (4)$$

where K , U , and W are kinetic energy, total strain energy, and work done by external forces, respectively. According to strain gradient theory, strain energy of the micro-plate is written as

$$U = \frac{1}{2} \int_{\Omega} \left(\sigma_{ij} \varepsilon_{ij} + p_i \gamma_i + \tau_{ijk}^{(1)} \eta_{ijk}^{(1)} + m_{ij}^s \chi_{ij}^s \right) dV, \quad (5)$$

where σ_{ij} is stress; ε_{ij} is strain; p_i , $\tau_{ijk}^{(1)}$, m_{ij}^s are higher order stress tensors; γ_i denotes dilatation gradient

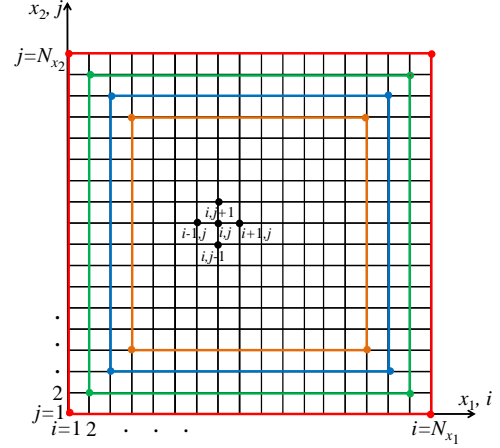


Fig. 2 Discretization of the mid-plane

vector; $\eta_{ijk}^{(1)}$ represents deviatoric stretch gradient tensor; χ_{ij}^s is symmetric curvature tensor; and Ω is volume. Kinetic energy and work are of the forms

$$K = \frac{1}{2} \int_{\Omega} \rho \left\{ \left(\frac{\partial u_1}{\partial t} \right)^2 + \left(\frac{\partial u_2}{\partial t} \right)^2 + \left(\frac{\partial u_3}{\partial t} \right)^2 \right\} dV, \quad (6a)$$

$$W = \int_A q w dA + \frac{1}{2} \int_A \left(P_{x_1} \left(\frac{\partial w}{\partial x_1} \right)^2 + P_{x_2} \left(\frac{\partial w}{\partial x_2} \right)^2 \right) dA. \quad (6b)$$

where ρ is mass density; $q(x_1, x_2)$ is distributed loading; A stands for mid-plane area; and P_{x_1} and P_{x_2} are axial in-plane buckling loads.

Deformation measures in Eq. (5) are defined by

$$\varepsilon_{ij} = \frac{1}{2} (u_{i,j} + u_{j,i}), \quad (7a)$$

$$\gamma_i = \varepsilon_{mm,i}, \quad (7b)$$

$$\eta_{ijk}^{(1)} = \frac{1}{3} (\varepsilon_{jk,i} + \varepsilon_{ki,j} + \varepsilon_{ij,k}) - \frac{1}{15} \delta_{ij} (\varepsilon_{mm,k} + 2\varepsilon_{mk,m}) - \frac{1}{15} \left\{ \delta_{jk} (\varepsilon_{mm,i} + 2\varepsilon_{mi,m}) + \delta_{ki} (\varepsilon_{mm,j} + 2\varepsilon_{mj,m}) \right\}, \quad (7c)$$

$$\chi_{ij}^s = \frac{1}{2} (e_{ipq} \varepsilon_{qj,p} + e_{jpq} \varepsilon_{qi,p}). \quad (7d)$$

e_{ijk} here designates alternating tensor, and δ_{ij} is Kronecker delta. Constitutive relations of strain gradient theory are expressed as

$$\begin{Bmatrix} \sigma_{11} \\ \sigma_{22} \\ \sigma_{12} \\ \sigma_{13} \\ \sigma_{23} \end{Bmatrix} = \frac{E}{1-\nu^2} \begin{bmatrix} 1 & \nu & 0 & 0 & 0 \\ \nu & 1 & 0 & 0 & 0 \\ 0 & 0 & 1-\nu & 0 & 0 \\ 0 & 0 & 0 & k_s(1-\nu) & 0 \\ 0 & 0 & 0 & 0 & k_s(1-\nu) \end{bmatrix} \begin{Bmatrix} \varepsilon_{11} \\ \varepsilon_{22} \\ \varepsilon_{12} \\ \varepsilon_{13} \\ \varepsilon_{23} \end{Bmatrix}, \quad (8a)$$

$$p_i = 2\mu l_0^2 \gamma_i, \quad \tau_{ijk}^{(1)} = 2\mu l_1^2 \eta_{ijk}^{(1)}, \quad m_{ij}^s = 2\mu l_2^2 \chi_{ij}^s. \quad (8b)$$

where E is modulus of elasticity, ν is Poisson's ratio, μ is shear modulus, k_s is shear correction factor, and l_i , $i = 0, 1, 2$, are length scale parameters. All of the material properties, including the length scale parameters l_i , $i = 0, 1, 2$, are assumed to be functions of the thickness coordinate x_3 . Shear correction factor is equal to unity in KPT and TSDT; and 5/6 in MPT.

Use of the Hamilton's principle given by Eq. (4) in conjunction with Eqs. (5)-(8) leads to following system of governing partial differential equations

$$\begin{aligned} \delta u : \\ & \left(-2A_{550} - \frac{4}{5} A_{551} \right) \frac{\partial^4 u}{\partial x_1^4} + \left(-\frac{8}{15} A_{551} - \frac{1}{4} A_{552} \right) \frac{\partial^4 u}{\partial x_2^4} \\ & + \left(-2A_{550} - \frac{4}{3} A_{551} - \frac{1}{4} A_{552} \right) \frac{\partial^4 u}{\partial x_1^2 \partial x_2^2} + A_{11} \frac{\partial^2 u}{\partial x_1^2} \\ & + A_{55} \frac{\partial^2 u}{\partial x_2^2} + \left(-2A_{550} - \frac{4}{15} A_{551} + \frac{1}{4} A_{552} \right) \frac{\partial^4 v}{\partial x_1^3 \partial x_2} \\ & + \left(-2A_{550} - \frac{4}{15} A_{551} + \frac{1}{4} A_{552} \right) \frac{\partial^4 v}{\partial x_1 \partial x_2^3} \\ & + (A_{55} + A_{L11}) \frac{\partial^2 v}{\partial x_1 \partial x_2} \\ & + \left(-2F_{470} + 2B_{550} + \frac{4}{5} B_{551} - \frac{4}{5} F_{471} \right) \frac{\partial^5 w}{\partial x_1^5} \\ & + \left(4B_{550} - 4F_{470} + \frac{8}{5} B_{551} - \frac{8}{5} F_{471} \right) \frac{\partial^5 w}{\partial x_1^3 \partial x_2^2} \\ & + \left(-2F_{470} + 2B_{550} + \frac{4}{5} B_{551} - \frac{4}{5} F_{471} \right) \frac{\partial^5 w}{\partial x_1 \partial x_2^4} \\ & + \left(F_{11} - B_{11} + \frac{2}{5} F_{671} \right) \frac{\partial^3 w}{\partial x_1^3} + \left(F_{11} - B_{11} + \frac{2}{5} F_{671} \right) \frac{\partial^3 w}{\partial x_1 \partial x_2^2} \\ & + \left(-2F_{470} - \frac{4}{5} F_{471} \right) \frac{\partial^4 \phi_1}{\partial x_1^4} + \left(-\frac{8}{15} F_{471} - \frac{1}{4} F_{472} \right) \frac{\partial^4 \phi_1}{\partial x_2^4} \\ & + \left(-2F_{470} - \frac{4}{3} F_{471} - \frac{1}{4} F_{472} \right) \frac{\partial^4 \phi_1}{\partial x_1^2 \partial x_2^2} \\ & + \left(F_{11} + \frac{2}{5} F_{671} \right) \frac{\partial^2 \phi_1}{\partial x_1^2} + \left(F_{47} + \frac{2}{15} F_{671} + \frac{1}{4} F_{672} \right) \frac{\partial^2 \phi_1}{\partial x_2^2} \\ & + \left(-2F_{470} - \frac{4}{15} F_{471} + \frac{1}{4} F_{472} \right) \frac{\partial^4 \phi_2}{\partial x_1^3 \partial x_2} \\ & + \left(-2F_{470} - \frac{4}{15} F_{471} + \frac{1}{4} F_{472} \right) \frac{\partial^4 \phi_2}{\partial x_1 \partial x_2^3} \\ & + \left(F_{L11} + F_{47} + \frac{4}{15} F_{671} - \frac{1}{4} F_{672} \right) \frac{\partial^2 \phi_2}{\partial x_1 \partial x_2} \\ & = I_0 \frac{\partial^2 u}{\partial t^2} + (I_3 - I_1) \frac{\partial^3 w}{\partial x_1 \partial t^2} + I_3 \frac{\partial^2 \phi_1}{\partial t^2}, \end{aligned} \quad (9a)$$

$\delta v :$

$$\begin{aligned} & \left(-2A_{550} - \frac{4}{15} A_{551} + \frac{1}{4} A_{552} \right) \frac{\partial^4 u}{\partial x_1^3 \partial x_2} + \left(-2A_{550} - \frac{4}{15} A_{551} \right. \\ & \left. + \frac{1}{4} A_{552} \right) \frac{\partial^4 u}{\partial x_1 \partial x_2^3} + (A_{55} + A_{L11}) \frac{\partial^2 u}{\partial x_1 \partial x_2} \\ & + \left(-\frac{8}{15} A_{551} - \frac{1}{4} A_{552} \right) \frac{\partial^4 v}{\partial x_1^4} + \left(-2A_{550} - \frac{4}{5} A_{551} \right) \frac{\partial^4 v}{\partial x_2^4} \\ & + \left(-2A_{550} - \frac{4}{3} A_{551} - \frac{1}{4} A_{552} \right) \frac{\partial^4 v}{\partial x_1^2 \partial x_2^2} + A_{55} \frac{\partial^2 v}{\partial x_1^2} \\ & + A_{11} \frac{\partial^2 v}{\partial x_2^2} + \left(-2F_{470} + 2B_{550} + \frac{4}{5} B_{551} - \frac{4}{5} F_{471} \right) \frac{\partial^5 w}{\partial x_2^5} \\ & + \left(2B_{550} + \frac{4}{5} B_{551} - 2F_{470} - \frac{4}{5} F_{471} \right) \frac{\partial^5 w}{\partial x_1^4 \partial x_2} \\ & + \left(4B_{550} + \frac{8}{5} B_{551} - 4F_{470} - \frac{8}{5} F_{471} \right) \frac{\partial^5 w}{\partial x_1^2 \partial x_2^3} \\ & + \left(F_{11} - B_{11} + \frac{2}{5} F_{671} \right) \frac{\partial^3 w}{\partial x_2^3} \\ & + \left(F_{11} - B_{11} + \frac{2}{5} F_{671} \right) \frac{\partial^3 w}{\partial x_1^2 \partial x_2} + \left(-2F_{470} - \frac{4}{15} F_{471} \right. \\ & \left. + \frac{1}{4} F_{472} \right) \frac{\partial^4 \phi_1}{\partial x_1^3 \partial x_2} + \left(-2F_{470} - \frac{4}{15} F_{471} + \frac{1}{4} F_{472} \right) \frac{\partial^4 \phi_1}{\partial x_1 \partial x_2^3} \\ & + \left(F_{L11} + F_{47} + \frac{4}{15} F_{671} - \frac{1}{4} F_{672} \right) \frac{\partial^2 \phi_1}{\partial x_1 \partial x_2} \\ & + \left(-\frac{8}{15} F_{471} - \frac{1}{4} F_{472} \right) \frac{\partial^4 \phi_2}{\partial x_1^4} + \left(-2F_{470} - \frac{4}{5} F_{471} \right) \frac{\partial^4 \phi_2}{\partial x_2^4} \\ & + \left(-2F_{470} - \frac{4}{3} F_{471} - \frac{1}{4} F_{472} \right) \frac{\partial^4 \phi_2}{\partial x_1^2 \partial x_2^2} \\ & + \left(F_{47} + \frac{2}{15} F_{671} + \frac{1}{4} F_{672} \right) \frac{\partial^2 \phi_2}{\partial x_1^2} + \left(F_{11} + \frac{2}{5} F_{671} \right) \frac{\partial^2 \phi_2}{\partial x_2^2} \\ & = I_0 \frac{\partial^2 v}{\partial t^2} + (I_3 - I_1) \frac{\partial^3 w}{\partial x_2 \partial t^2} + I_3 \frac{\partial^2 \phi_2}{\partial t^2}, \end{aligned} \quad (9b)$$

$\delta w :$

$$\begin{aligned} & \left(-2B_{550} + 2F_{470} - \frac{4}{5} B_{551} + \frac{4}{5} F_{471} \right) \frac{\partial^5 u}{\partial x_1^5} \\ & + \left(-4B_{550} + 4F_{470} - \frac{8}{5} B_{551} + \frac{8}{5} F_{471} \right) \frac{\partial^5 u}{\partial x_1^3 \partial x_2^2} \\ & + \left(-2B_{550} + 2F_{470} - \frac{4}{5} B_{551} + \frac{4}{5} F_{471} \right) \frac{\partial^5 u}{\partial x_1 \partial x_2^4} \\ & + \left(B_{11} - F_{11} - \frac{2}{5} F_{671} \right) \frac{\partial^3 u}{\partial x_1^3} + \left(B_{11} - F_{11} - \frac{2}{5} F_{671} \right) \frac{\partial^3 u}{\partial x_1 \partial x_2^2} \\ & + \left(-2B_{550} + 2F_{470} - \frac{4}{5} B_{551} + \frac{4}{5} F_{471} \right) \frac{\partial^5 v}{\partial x_2^5} \\ & + \left(-2B_{550} + 2F_{470} - \frac{4}{5} B_{551} + \frac{4}{5} F_{471} \right) \frac{\partial^5 v}{\partial x_1^4 \partial x_2} \\ & + \left(-4B_{550} + 4F_{470} - \frac{8}{5} B_{551} + \frac{8}{5} F_{471} \right) \frac{\partial^5 v}{\partial x_1^2 \partial x_2^3} \\ & + \left(B_{11} - F_{11} - \frac{2}{5} F_{671} \right) \frac{\partial^3 v}{\partial x_2^3} + \left(B_{11} - F_{11} - \frac{2}{5} F_{671} \right) \frac{\partial^3 v}{\partial x_1^2 \partial x_2} \end{aligned} \quad (9c)$$

$$\begin{aligned}
 & + \left(2D_{550} + 2F_{440} - 4F_{480} + \frac{4}{5}D_{551} + \frac{4}{5}F_{441} - \frac{8}{5}F_{481} \right) \frac{\partial^6 w}{\partial x_1^6} \\
 & + \left(2D_{550} + 2F_{440} - 4F_{480} + \frac{4}{5}D_{551} + \frac{4}{5}F_{441} - \frac{8}{5}F_{481} \right) \frac{\partial^6 w}{\partial x_2^6} \\
 & + \left(6D_{550} + 6F_{440} - 12F_{480} + \frac{12}{5}D_{551} + \frac{12}{5}F_{441} \right. \\
 & \left. - \frac{24}{5}F_{481} \right) \frac{\partial^6 w}{\partial x_1^4 \partial x_2^2} + \left(6D_{550} + 6F_{440} - 12F_{480} + \frac{12}{5}D_{551} \right. \\
 & \left. + \frac{12}{5}F_{441} - \frac{24}{5}F_{481} \right) \frac{\partial^6 w}{\partial x_1^2 \partial x_2^4} + (-D_{11} + 2F_{22} - F_{33} - 2A_{550} \\
 & - 2F_{550} + 4F_{570} - \frac{8}{15}A_{551} - \frac{4}{5}F_{461} - \frac{32}{15}F_{551} + \frac{32}{15}F_{571} \\
 & + \frac{4}{5}F_{681} - A_{552} - \frac{1}{4}F_{552} + F_{572}) \frac{\partial^4 w}{\partial x_1^4} + (-D_{11} + 2F_{22} - F_{33} \\
 & - 2A_{550} - 2F_{550} + 4F_{570} - \frac{8}{15}A_{551} - \frac{4}{5}F_{461} - \frac{32}{15}F_{551} \\
 & + \frac{32}{15}F_{571} + \frac{4}{5}F_{681} - A_{552} - \frac{1}{4}F_{552} + F_{572}) \frac{\partial^4 w}{\partial x_2^4} \\
 & + (-2D_{11} + 4F_{22} - 2F_{33} - 4A_{550} - 4F_{550} + 8F_{570} - \frac{16}{15}A_{551} \\
 & - \frac{8}{5}F_{461} - \frac{64}{15}F_{551} + \frac{64}{15}F_{571} + \frac{8}{5}F_{681} - 2A_{552} - \frac{1}{2}F_{552} \\
 & + 2F_{572}) \frac{\partial^4 w}{\partial x_1^2 \partial x_2^2} + \left(k_s F_{55} + \frac{8}{15}F_{661} + \frac{1}{4}F_{662} \right) \frac{\partial^2 w}{\partial x_1^2} \\
 & + \left(k_s F_{55} + \frac{8}{15}F_{661} + \frac{1}{4}F_{662} \right) \frac{\partial^2 w}{\partial x_2^2} \\
 & + \left(2F_{440} - 2F_{480} + \frac{4}{5}F_{441} - \frac{4}{5}F_{481} \right) \frac{\partial^5 \phi_1}{\partial x_1^5} \\
 & + \left(4F_{440} - 4F_{480} + \frac{8}{5}F_{441} - \frac{8}{5}F_{481} \right) \frac{\partial^5 \phi_1}{\partial x_1^3 \partial x_2^2} \\
 & + \left(2F_{440} - 2F_{480} + \frac{4}{5}F_{441} - \frac{4}{5}F_{481} \right) \frac{\partial^5 \phi_1}{\partial x_1 \partial x_2^4} \\
 & + \left(F_{22} - F_{33} - 2F_{550} + 2F_{570} - \frac{4}{5}F_{461} - \frac{32}{15}F_{551} + \frac{16}{15}F_{571} \right. \\
 & \left. + \frac{2}{5}F_{681} - \frac{1}{4}F_{552} + \frac{1}{2}F_{572} \right) \frac{\partial^3 \phi_1}{\partial x_1^3} \\
 & + \left(F_{22} - F_{33} - 2F_{550} + 2F_{570} - \frac{4}{5}F_{461} \right. \\
 & \left. - \frac{32}{15}F_{551} + \frac{16}{15}F_{571} + \frac{2}{5}F_{681} - \frac{1}{4}F_{552} + \frac{1}{2}F_{572} \right) \frac{\partial^3 \phi_1}{\partial x_1 \partial x_2^2} \\
 & + \left(k_s F_{55} + \frac{8}{15}F_{661} + \frac{1}{4}F_{662} \right) \frac{\partial \phi_1}{\partial x_1} \\
 & + \left(2F_{440} - 2F_{480} + \frac{4}{5}F_{441} - \frac{4}{5}F_{481} \right) \frac{\partial^5 \phi_2}{\partial x_2^5} \\
 & + \left(2F_{440} - 2F_{480} + \frac{4}{5}F_{441} - \frac{4}{5}F_{481} \right) \frac{\partial^5 \phi_2}{\partial x_1^4 \partial x_2} \\
 & + \left(4F_{440} - 4F_{480} + \frac{8}{5}F_{441} - \frac{8}{5}F_{481} \right) \frac{\partial^5 \phi_2}{\partial x_1^2 \partial x_2^3} \\
 & + \left(F_{22} - F_{33} - 2F_{550} + 2F_{570} - \frac{4}{5}F_{461} - \frac{32}{15}F_{551} \right. \\
 & \left. + \frac{16}{15}F_{571} + \frac{2}{5}F_{681} - \frac{1}{4}F_{552} + \frac{1}{2}F_{572} \right) \frac{\partial^3 \phi_2}{\partial x_2^3}
 \end{aligned}$$

$$\begin{aligned}
 & + \left(F_{22} - F_{33} - 2F_{550} + 2F_{570} - \frac{4}{5}F_{461} - \frac{32}{15}F_{551} \right. \\
 & \left. + \frac{16}{15}F_{571} + \frac{2}{5}F_{681} - \frac{1}{4}F_{552} + \frac{1}{2}F_{572} \right) \frac{\partial^3 \phi_2}{\partial x_1^2 \partial x_2} \\
 & + \left(k_s F_{55} + \frac{8}{15}F_{661} + \frac{1}{4}F_{662} \right) \frac{\partial \phi_2}{\partial x_2} + q \\
 & - P_{x_1} \frac{\partial^2 w}{\partial x_1^2} - P_{x_2} \frac{\partial^2 w}{\partial x_2^2} = (I_1 - I_3) \frac{\partial^3 u}{\partial x_1 \partial t^2} + (I_1 - I_3) \frac{\partial^3 v}{\partial x_2 \partial t^2} \\
 & + (2I_4 - I_2 - I_5) \frac{\partial^4 w}{\partial x_1^2 \partial t^2} + (2I_4 - I_2 - I_5) \frac{\partial^4 w}{\partial x_2^2 \partial t^2} \\
 & + I_0 \frac{\partial^2 w}{\partial t^2} + (I_4 - I_5) \frac{\partial^3 \phi_1}{\partial x_1 \partial t^2} + (I_4 - I_5) \frac{\partial^3 \phi_2}{\partial x_2 \partial t^2},
 \end{aligned}$$

$\delta \phi_1 :$

$$\begin{aligned}
 & \left(-2F_{470} - \frac{4}{5}F_{471} \right) \frac{\partial^4 u}{\partial x_1^4} + \left(-\frac{8}{15}F_{471} - \frac{1}{4}F_{472} \right) \frac{\partial^4 u}{\partial x_2^4} \\
 & + \left(-2F_{470} - \frac{4}{3}F_{471} - \frac{1}{4}F_{472} \right) \frac{\partial^4 u}{\partial x_1^2 \partial x_2^2} \\
 & + \left(F_{11} + \frac{2}{5}F_{671} \right) \frac{\partial^2 u}{\partial x_1^2} + \left(F_{47} + \frac{2}{15}F_{671} + \frac{1}{4}F_{672} \right) \frac{\partial^2 u}{\partial x_2^2} \\
 & + \left(-2F_{470} - \frac{4}{15}F_{471} + \frac{1}{4}F_{472} \right) \frac{\partial^4 v}{\partial x_1^3 \partial x_2} \\
 & + \left(-2F_{470} - \frac{4}{15}F_{471} + \frac{1}{4}F_{472} \right) \frac{\partial^4 v}{\partial x_1 \partial x_2^3} \\
 & + \left(F_{L11} + F_{47} + \frac{4}{15}F_{671} - \frac{1}{4}F_{672} \right) \frac{\partial^2 v}{\partial x_1 \partial x_2} + (-2F_{440} \\
 & + 2F_{480} - \frac{4}{5}F_{441} + \frac{4}{5}F_{481}) \frac{\partial^5 w}{\partial x_1^5} + (-4F_{440} + 4F_{480} \\
 & - \frac{8}{5}F_{441} + \frac{8}{5}F_{481}) \frac{\partial^5 w}{\partial x_1^3 \partial x_2^2} + \left(-2F_{440} + 2F_{480} - \frac{4}{5}F_{441} \right. \\
 & \left. + \frac{4}{5}F_{481} \right) \frac{\partial^5 w}{\partial x_1 \partial x_2^4} + \left(-F_{22} + F_{33} + 2F_{550} - 2F_{570} + \frac{4}{5}F_{461} \right. \\
 & \left. + \frac{32}{15}F_{551} - \frac{16}{15}F_{571} - \frac{2}{5}F_{681} + \frac{1}{4}F_{552} - \frac{1}{2}F_{572} \right) \frac{\partial^3 w}{\partial x_1^3} \\
 & + \left(-F_{22} + F_{33} + 2F_{550} - 2F_{570} + \frac{4}{5}F_{461} + \frac{32}{15}F_{551} \right. \\
 & \left. - \frac{16}{15}F_{571} - \frac{2}{5}F_{681} + \frac{1}{4}F_{552} - \frac{1}{2}F_{572} \right) \frac{\partial^3 w}{\partial x_1 \partial x_2^2} \\
 & + \left(-k_s F_{55} - \frac{8}{15}F_{661} - \frac{1}{4}F_{662} \right) \frac{\partial w}{\partial x_1} \\
 & + \left(-2F_{440} - \frac{4}{5}F_{441} \right) \frac{\partial^4 \phi_1}{\partial x_1^4} + \left(-\frac{8}{15}F_{441} - \frac{1}{4}F_{442} \right) \frac{\partial^4 \phi_1}{\partial x_2^4} \\
 & + \left(-2F_{440} - \frac{4}{3}F_{441} - \frac{1}{4}F_{442} \right) \frac{\partial^4 \phi_1}{\partial x_1^2 \partial x_2^2} \\
 & + \left(F_{33} + 2F_{550} + \frac{4}{5}F_{461} + \frac{32}{15}F_{551} + \frac{1}{4}F_{552} \right) \frac{\partial^2 \phi_1}{\partial x_1^2}
 \end{aligned} \tag{9d}$$

$$\begin{aligned}
& + \left(F_{44} + \frac{4}{15} F_{461} + \frac{4}{3} F_{551} + \frac{1}{2} F_{462} + F_{552} \right) \frac{\partial^2 \phi_1}{\partial x_2^2} \\
& + \left(-k_s F_{55} - \frac{8}{15} F_{661} - \frac{1}{4} F_{662} \right) \phi_1 + \left(-2F_{440} - \frac{4}{15} F_{441} \right. \\
& + \left. \frac{1}{4} F_{442} \right) \frac{\partial^4 \phi_2}{\partial x_1^3 \partial x_2} + \left(-2F_{440} - \frac{4}{15} F_{441} + \frac{1}{4} F_{442} \right) \frac{\partial^4 \phi_2}{\partial x_1 \partial x_2^3} \\
& + \left(F_{L33} + F_{44} + 2F_{550} + \frac{8}{15} F_{461} + \frac{4}{5} F_{551} - \frac{1}{2} F_{462} \right. \\
& \left. - \frac{3}{4} F_{552} \right) \frac{\partial^2 \phi_2}{\partial x_1 \partial x_2} = I_3 \frac{\partial^2 u}{\partial t^2} + (I_5 - I_4) \frac{\partial^3 w}{\partial x_1 \partial t^2} + I_5 \frac{\partial^2 \phi_1}{\partial t^2} \\
\delta \phi_2 : \\
& \left(-2F_{470} - \frac{4}{15} F_{471} + \frac{1}{4} F_{472} \right) \frac{\partial^4 u}{\partial x_1^3 \partial x_2} \\
& + \left(-2F_{470} - \frac{4}{15} F_{471} + \frac{1}{4} F_{472} \right) \frac{\partial^4 u}{\partial x_1 \partial x_2^3} \\
& + \left(F_{L11} + F_{47} + \frac{4}{15} F_{671} - \frac{1}{4} F_{672} \right) \frac{\partial^2 u}{\partial x_1 \partial x_2} \\
& + \left(-\frac{8}{15} F_{471} - \frac{1}{4} F_{472} \right) \frac{\partial^4 v}{\partial x_1^4} + \left(-2F_{470} - \frac{4}{5} F_{471} \right) \frac{\partial^4 v}{\partial x_2^4} \\
& + \left(-2F_{470} - \frac{4}{3} F_{471} - \frac{1}{4} F_{472} \right) \frac{\partial^4 v}{\partial x_1^2 \partial x_2^2} \\
& + \left(F_{47} + \frac{2}{15} F_{671} + \frac{1}{4} F_{672} \right) \frac{\partial^2 v}{\partial x_1^2} + \left(F_{11} + \frac{2}{5} F_{671} \right) \frac{\partial^2 v}{\partial x_2^2} \\
& + \left(-2F_{440} + 2F_{480} - \frac{4}{5} F_{441} + \frac{4}{5} F_{481} \right) \frac{\partial^5 w}{\partial x_2^5} \\
& + \left(-4F_{440} + 4F_{480} - \frac{8}{5} F_{441} + \frac{8}{5} F_{481} \right) \frac{\partial^5 w}{\partial x_1^2 \partial x_2^3} \\
& + \left(-2F_{440} + 2F_{480} - \frac{4}{5} F_{441} + \frac{4}{5} F_{481} \right) \frac{\partial^5 w}{\partial x_1^4 \partial x_2} \\
& + \left(-F_{22} + F_{33} + 2F_{550} - 2F_{570} + \frac{4}{5} F_{461} + \frac{32}{15} F_{551} \right. \\
& \left. - \frac{16}{15} F_{571} - \frac{2}{5} F_{681} + \frac{1}{4} F_{552} - \frac{1}{2} F_{572} \right) \frac{\partial^3 w}{\partial x_2^3} \\
& + \left(-F_{22} + F_{33} + 2F_{550} - 2F_{570} + \frac{4}{5} F_{461} \right. \\
& \left. + \frac{32}{15} F_{551} - \frac{16}{15} F_{571} - \frac{2}{5} F_{681} + \frac{1}{4} F_{552} - \frac{1}{2} F_{572} \right) \frac{\partial^3 w}{\partial x_1^2 \partial x_2} \\
& + \left(-k_s F_{55} - \frac{8}{15} F_{661} - \frac{1}{4} F_{662} \right) \frac{\partial w}{\partial x_2} \\
& + \left(-2F_{440} - \frac{4}{15} F_{441} + \frac{1}{4} F_{442} \right) \frac{\partial^4 \phi_1}{\partial x_1^3 \partial x_2} \\
& + \left(-2F_{440} - \frac{4}{15} F_{441} + \frac{1}{4} F_{442} \right) \frac{\partial^4 \phi_1}{\partial x_1 \partial x_2^3}
\end{aligned} \tag{9e}$$

$$\begin{aligned}
& + \left(F_{L33} + F_{44} + 2F_{550} + \frac{8}{15} F_{461} + \frac{4}{5} F_{551} \right. \\
& \left. - \frac{1}{2} F_{462} - \frac{3}{4} F_{552} \right) \frac{\partial^2 \phi_1}{\partial x_1 \partial x_2} + \left(-\frac{8}{15} F_{441} - \frac{1}{4} F_{442} \right) \frac{\partial^4 \phi_2}{\partial x_1^4} \\
& + \left(-2F_{440} - \frac{4}{5} F_{441} \right) \frac{\partial^4 \phi_2}{\partial x_2^4} \\
& + \left(-2F_{440} - \frac{4}{3} F_{441} - \frac{1}{4} F_{442} \right) \frac{\partial^4 \phi_2}{\partial x_1^2 \partial x_2^2} \\
& + \left(F_{44} + \frac{4}{15} F_{461} + \frac{4}{3} F_{551} + \frac{1}{2} F_{462} + F_{552} \right) \frac{\partial^2 \phi_2}{\partial x_1^2} \\
& + \left(F_{33} + 2F_{550} + \frac{4}{5} F_{461} + \frac{32}{15} F_{551} + \frac{1}{4} F_{552} \right) \frac{\partial^2 \phi_2}{\partial x_2^2} \\
& + \left(-k_s F_{55} - \frac{8}{15} F_{661} - \frac{1}{4} F_{662} \right) \phi_2 \\
& = I_3 \frac{\partial^2 v}{\partial t^2} + (I_5 - I_4) \frac{\partial^3 w}{\partial x_2 \partial t^2} + I_5 \frac{\partial^2 \phi_2}{\partial t^2}.
\end{aligned}$$

Note that in static bending problems time derivatives on the right sides and terms involving buckling loads are set to zero. In free vibration analysis, there is no external forcing. Buckling formulation does not include any time derivatives as well as distributed loading. Application of Hamilton's principle also yields the boundary conditions. However, because of their rather lengthy forms, the boundary conditions are not provided here. The coefficients in Eq. (9) are as follows

$$\begin{aligned}
& \{A_{11}, B_{11}, D_{11}, F_{11}, F_{22}, F_{33}\} \\
& = \int_{-\frac{h}{2}}^{\frac{h}{2}} \frac{E(x_3)}{1-\nu(x_3)} \{1, x_3, x_3^2, f, x_3 f, f^2\} dx_3,
\end{aligned} \tag{10a}$$

$$\begin{aligned}
& \{A_{211}, B_{211}, D_{211}, F_{211}, F_{222}, F_{233}\} \\
& = \int_{-\frac{h}{2}}^{\frac{h}{2}} \frac{E(x_3)\nu(x_3)}{1-\nu(x_3)} \{1, x_3, x_3^2, f, x_3 f, f^2\} dx_3,
\end{aligned} \tag{10b}$$

$$\begin{aligned}
& \{A_{55}, B_{55}, D_{55}, F_{44}, F_{46}, F_{47}, F_{48}, F_{55}, F_{57}, F_{66}, F_{67}, F_{68}\} \\
& = \int_{-\frac{h}{2}}^{\frac{h}{2}} \frac{E(x_3)}{2(1+\nu(x_3))} \{1, x_3, x_3^2, f^2, ff'', f, x_3 f, f^2, f', \\
& f'^2, f'', x_3 f''\} dx_3,
\end{aligned} \tag{10c}$$

$$\begin{aligned}
& \{A_{550}, B_{550}, D_{550}, F_{440}, F_{460}, F_{470}, F_{480}, F_{550}, \\
& F_{570}, F_{660}, F_{670}, F_{680}\} = \int_{-\frac{h}{2}}^{\frac{h}{2}} \frac{E(x_3)I_0(x_3)}{2(1+\nu(x_3))} \{1, x_3, x_3^2, \\
& f^2, ff'', f, x_3 f, f^2, f', f'^2, f'', x_3 f''\} dx_3,
\end{aligned} \tag{10d}$$

$$\begin{aligned}
& \{A_{551}, B_{551}, D_{551}, F_{441}, F_{461}, F_{471}, F_{481}, F_{551}, \\
& F_{571}, F_{661}, F_{671}, F_{681}\} = \int_{-\frac{h}{2}}^{\frac{h}{2}} \frac{E(x_3)I_1(x_3)}{2(1+\nu(x_3))} \{1, x_3, x_3^2, \\
& f^2, ff'', f, x_3 f, f^2, f', f'^2, f'', x_3 f''\} dx_3,
\end{aligned} \tag{10e}$$

$$\begin{aligned}
& \{A_{552}, B_{552}, D_{552}, F_{442}, F_{462}, F_{472}, F_{482}, F_{552}, \\
& F_{572}, F_{662}, F_{672}, F_{682}\} = \int_{-\frac{h}{2}}^{\frac{h}{2}} \frac{E(x_3)I_2(x_3)}{2(1+\nu(x_3))} \{1, x_3, x_3^2, \\
& f^2, ff'', f, x_3 f, f^2, f', f'^2, f'', x_3 f''\} dx_3,
\end{aligned} \tag{10f}$$

$$\begin{aligned}
& \{I_0, I_1, I_2, I_3, I_4, I_5\} \\
& = \int_{-\frac{h}{2}}^{\frac{h}{2}} \rho(x_3) \{1, x_3, x_3^2, f, x_3 f, f^2\} dx_3.
\end{aligned} \tag{10g}$$

3. Numerical solution

Differential quadrature method is employed to solve the system comprising governing partial differential equations and boundary conditions. The technique, which was originally proposed by Bellman and Casti (1971), is based on approximating derivative of a function by a weighted sum of functional values. m^{th} derivative of a function $z(x, t)$ with respect to x at a point x_i is represented as

$$\frac{\partial^m z(x, t)}{\partial x^m} \Big|_{x=x_i} = \sum_{j=1}^N c_{ij}^{(m)} z(x_j, t), \quad i = 1, 2, \dots, N \quad (11)$$

N here is the number of nodes, and $c_{ij}^{(m)}$ are the weighting coefficients for the m^{th} derivative. The coefficients are available in the book by Shu (2000). Fig. 2 depicts discretization of the mid-plane of the FGM micro-plate. N_{x_1} and N_{x_2} in the figure are numbers of grid points in x_1 and x_2 directions, respectively.

An important factor influencing stability of DQM is the distribution of grid points. We used Chebyshev-Gauss-Lobatto points, which result in a more stable procedure compared to uniform grid points (Ng *et al.* 2009). Chebyshev-Gauss-Lobatto points for a two dimensional setting $0 \leq x_1 \leq 1$ and $0 \leq x_2 \leq 1$, are given by

$$x_{1i} = \frac{1}{2} \left\{ 1 - \cos \left(\frac{\pi(i-1)}{N_{x_1} - 1} \right) \right\}, \quad i = 1, 2, \dots, N_{x_1}, \quad (12)$$

$$x_{2j} = \frac{1}{2} \left\{ 1 - \cos \left(\frac{\pi(j-1)}{N_{x_2} - 1} \right) \right\}, \quad j = 1, 2, \dots, N_{x_2}.$$

3.1 Static bending

For a rectangular FGM micro-plate under static loading, unknown generalized displacement vector \mathbf{d} is defined as follows

$$\mathbf{d} = \left\{ \{u_p\}^T, \{v_p\}^T, \{w_p\}^T, \{\phi_{1p}\}^T, \{\phi_{2p}\}^T \right\}^T, \quad (13)$$

for $p = 1, 2, \dots, N_{x_1} \times N_{x_2}$,

where $\{u_p\}$, $\{v_p\}$, $\{w_p\}$, $\{\phi_{1p}\}$ and $\{\phi_{2p}\}$ are unknown vectors with $N_{x_1} \times N_{x_2}$ elements. Eliminating in-plane forces and the terms including time derivatives; and utilizing DQM, governing equations and boundary conditions are recast into the following matrix form

$$\mathbf{D}\mathbf{d} + \mathbf{Q} = \mathbf{0}, \quad (14)$$

in which \mathbf{D} is coefficient matrix associated with grid points, and \mathbf{Q} is forcing vector resulting from distributed loading.

3.2 Free vibrations

In free vibration analysis, all external forces are equated to zero. Dynamic displacement vector is defined by

$$\mathbf{d} = \mathbf{d}^* e^{i\omega t}, \quad (15)$$

where ω represents natural frequency and \mathbf{d}^* is mode shape vector expressed as

$$\mathbf{d}^* = \left\{ \{u_p^*\}^T, \{v_p^*\}^T, \{w_p^*\}^T, \{\phi_{1p}^*\}^T, \{\phi_{2p}^*\}^T \right\}^T, \quad (16)$$

for $p = 1, 2, \dots, N_{x_1} \times N_{x_2}$.

Substitution of Eq. (15) into governing equations leads to

$$\mathbf{D}_b \mathbf{d}^{*e} + \mathbf{D}_d \mathbf{d}^{*i} - \omega^2 \mathbf{M} \mathbf{d}^{*i} = \mathbf{0}, \quad (17)$$

where \mathbf{d}^{*e} and \mathbf{d}^{*i} are dynamic displacement vectors for boundary and internal points, respectively; \mathbf{D}_b and \mathbf{D}_d are coefficient matrices associated with boundary and internal points; and \mathbf{M} is mass matrix. Using Eq. (15) and boundary conditions one finds

$$\mathbf{B}_b \mathbf{d}^{*e} + \mathbf{B}_d \mathbf{d}^{*i} = \mathbf{0}. \quad (18)$$

\mathbf{B}_b and \mathbf{B}_d are coefficient matrices obtained from boundary conditions associated with boundary and internal points, respectively. Combining Eqs. (17) and (18), we derive the eigenvalue problem

$$\{\mathbf{K} - \omega^2 \mathbf{M}\} \mathbf{d}^{*i} = \mathbf{0}. \quad (19)$$

\mathbf{K} here is stiffness matrix given by

$$\mathbf{K} = -\mathbf{D}_b \mathbf{B}_b^{-1} \mathbf{B}_d + \mathbf{D}_d. \quad (20)$$

3.3 Buckling

In buckling analysis, we considered equiaxial loading and set $P_{x_1} = P_{x_2} = P$. Thus, buckling forces acting in x_1 and x_2 directions are the only external forces imposed on the micro-plate. Similar to the vibration formulation, buckling solution procedure leads to an eigenvalue problem. However, instead of mass matrix \mathbf{M} , a coefficient matrix \mathbf{X} is generated from the derivative terms $\partial^2 w / \partial x_1^2$ and $\partial^2 w / \partial x_2^2$. The eigenvalue problem is derived in the following form

$$\{\mathbf{K} - P\mathbf{X}\} \mathbf{d}_b^{*i} = \mathbf{0}. \quad (21)$$

The eigenvalue P computed from Eq. (21) is the critical buckling load of the rectangular FGM micro-plate, and \mathbf{d}_b^{*i} is mode shape vector for internal points.

4. Numerical results

The functionally graded rectangular micro-plate is assumed to be simply-supported in numerical analyses. General geometry of the micro-plate is shown in Fig. 1. Boundary conditions to be satisfied by the simply-supported

plate are as follows:

$$x_1 = 0, a:$$

$$\frac{\partial u}{\partial x_1} = v = w = \frac{\partial^2 w}{\partial x_1^2} = \frac{\partial \phi_1}{\partial x_1} = \phi_2 = 0, \quad (22a)$$

$$u \neq 0, \quad \frac{\partial v}{\partial x_1} \neq 0, \quad \frac{\partial w}{\partial x_1} \neq 0, \quad \phi_1 \neq 0, \quad \frac{\partial \phi_2}{\partial x_1} \neq 0, \quad (22b)$$

$$x_2 = 0, b:$$

$$u = \frac{\partial v}{\partial x_2} = w = \frac{\partial^2 w}{\partial x_2^2} = \phi_1 = \frac{\partial \phi_2}{\partial x_2} = 0, \quad (22c)$$

$$v \neq 0, \quad \frac{\partial u}{\partial x_2} \neq 0, \quad \frac{\partial w}{\partial x_2} \neq 0, \quad \frac{\partial \phi_1}{\partial x_2} \neq 0, \quad \phi_2 \neq 0. \quad (22d)$$

Boundary conditions are implemented similar to the implementation of boundary conditions in beams. If more than one condition is defined on a boundary, in order to implement the other boundary conditions, the closest grid points are used. For instance, for simply supported micro-plates, the boundary conditions are given in Eq. (22), where for w , three conditions are defined based on w , its first derivative $\partial w / \partial x_k$ and its second derivative $\partial^2 w / \partial x_k^2$. Boundary condition for w is implemented on the outer grid points designated by red color in Fig. 2. In order to implement the boundary condition for $\partial w / \partial x_k$ and $\partial^2 w / \partial x_k^2$, grid points shown by green and blue colors are used, respectively. However, as one moves from the outer edges of the boundary to the inner edges, the number of grid points decreases by 8 at each step. Therefore, after the implementation of derivative boundary conditions, $8+16=24$ boundary equations are missing. In order to fully implement the boundary conditions, required number of equations are employed on the orange grid points. However, it should be noted that $\partial w / \partial x_k$, and $\partial^2 w / \partial x_k^2$ for $k=1,2$ are automatically determined for corner points on the outer edges because $w=0$ on all grid points shown by red color. Therefore, it is not required to implement conditions related with derivatives of w for corner points indicated by red dots. Hence, $4+12=16$ boundary equations are defined by using 16 grid points on the orange boundary edge.

All mechanical properties, including the length scale parameters, are taken as functions of the thickness coordinate x_3 . The plate is 100% metal at $x_3 = -h/2$ and 100% ceramic at $x_3 = h/2$. Volume fractions of the constituent phases are expressed as

$$V_c(x_3) = (0.5 + x_3/h)^n, \quad V_c + V_m = 1. \quad (23)$$

Subscripts c and m stand for ceramic and metallic components, respectively; and n is volume fraction exponent. Material properties are represented as follows

$$E(x_3) = E_c V_c(x_3) + E_m V_m(x_3), \quad (24a)$$

Table 1 Comparisons of the dimensionless deflection (w_{max}/h) for a homogeneous micro-plate, $\nu = 0.3$, $b/a = 1.0$, $q = 1000 \text{ N/m}^2$

a/h		h/l		
		1.0	2.0	5.0
10	Present	3.3427E-5	8.0393E-5	2.0811E-4
	Ansari <i>et al.</i> (2015)	3.3211E-5	8.0250E-5	2.0834E-4
50	Present	0.0125	0.0412	0.1209
	Ansari <i>et al.</i> (2015)	0.0125	0.0413	0.1212

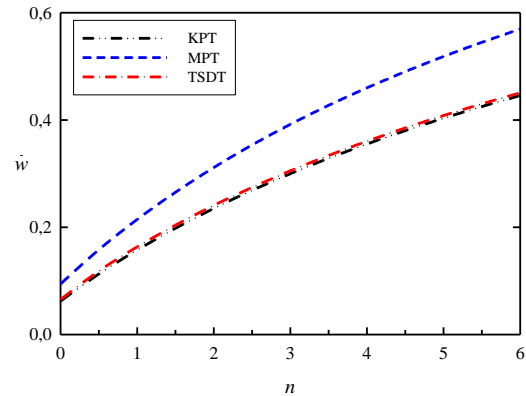


Fig. 3 Dimensionless maximum deflection, $l = 15 \mu\text{m}$, $l/h = 0.4$, $a/h = 10$, $b/a = 1.0$, $\beta = 2.0$, $q = 1 \text{ N/m}^2$

$$\nu(x_3) = \nu_c V_c(x_3) + \nu_m V_m(x_3), \quad (24b)$$

$$\rho(x_3) = \rho_c V_c(x_3) + \rho_m V_m(x_3), \quad (24c)$$

$$l_i(x_3) = l_{ic} V_c(x_3) + l_{im} V_m(x_3), \quad i = 0, 1, 2, \quad (24d)$$

where E is modulus of elasticity, ν is Poisson's ratio, ρ is density, and l_i , ($i=0,1,2$), are length scale parameters of strain gradient theory. The particular metallic and ceramic materials considered in computations are aluminum (Al) and silicon carbide (SiC) for which material properties are given as (Eshraghi *et al.* 2016)

$$E_c = 427 \text{ GPa}, \quad E_m = 70 \text{ GPa}, \quad (25a)$$

$$\nu_c = 0.17, \quad \nu_m = 0.3, \quad (25b)$$

$$\rho_c = 3100 \text{ kg/m}^3, \quad \rho_m = 2702 \text{ kg/m}^3. \quad (25c)$$

Since there is not sufficient characterization data in the literature on length scale parameters, approximate values are used for functionally graded small-scale structures (Gholami and Ansari 2016, Sahmani and Ansari 2013). In the present study, length scale parameters of the metallic phase are taken as $l_{0m} = l_{1m} = l_{2m} = l = 15 \mu\text{m}$; and those of the ceramic component are defined as $l_{0c} = l_{1c} = l_{2c} = \beta l$, where β is length scale parameter ratio. Note that when

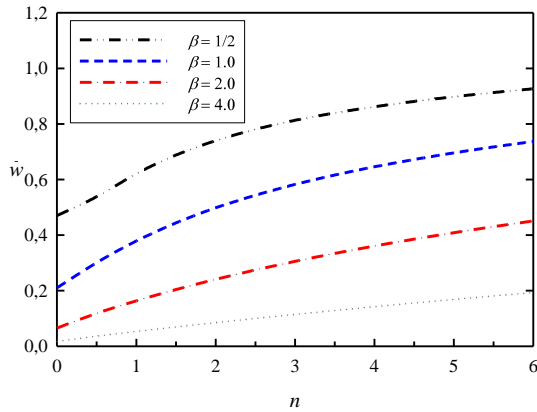


Fig. 4 Dimensionless maximum deflection, $l = 15 \mu\text{m}$, $l/h = 0.4$, $a/h = 10$, $b/a = 1.0$, $q = 1 \text{ N/m}^2$

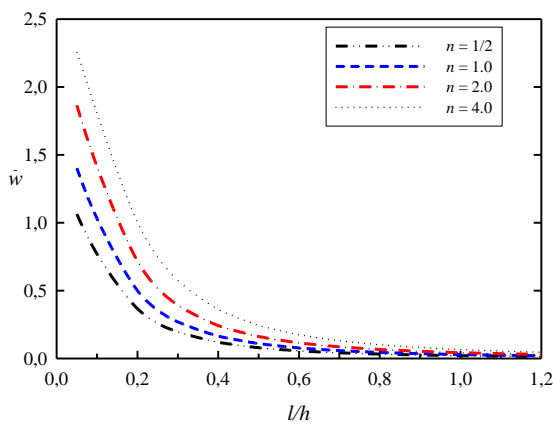


Fig. 5 Dimensionless maximum deflection, $h = 25 \mu\text{m}$, $a/h = 10$, $b/a = 1.0$, $\beta = 2.0$, $q = 1 \text{ N/m}^2$

$\beta = 1$, length scale parameters are constant within the micro-plate. Any positive β value other than unity implies spatial length scale parameter variations.

4.1 Static bending

In order to be able to verify the developed procedures, we first present some comparisons to the static bending results provided by Ansari *et al.* (2015). Table 1 tabulates comparisons regarding normalized maximum deflection w_{max}/h , of a simply-supported homogeneous micro-plate under uniform loading q . Maximum deflection occurs at the mid-point of the simply-supported plate. Material properties are given by

$$\begin{aligned} E &= 1.44 \text{ GPa}, \quad \rho = 1220 \text{ kg/m}^3, \\ l_0 = l_1 = l_2 = l &= 17.6 \mu\text{m}. \end{aligned} \quad (26)$$

The results are generated in accordance with Mindlin plate theory. The excellent agreement between the deflections is indicative of the high degree of accuracy attained by the application of the developed procedures.

Fig. 3 shows dimensionless maximum deflection \bar{w} for a functionally graded simply-supported micro-plate

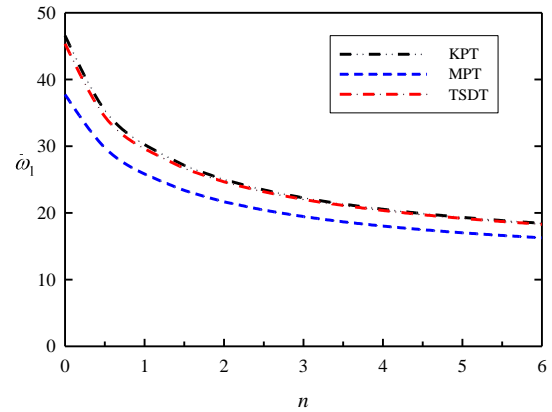


Fig. 6 First dimensionless transverse natural frequency, $l = 15 \mu\text{m}$, $l/h = 0.4$, $a/h = 10$, $b/a = 1.0$, $\beta = 2.0$

Table 2 Comparisons of the first natural frequency ω_1 (in MHz) for a homogeneous micro-plate, $\nu = 0.38$, $a/h = 10$, $b/a = 1.0$

	h/t				
	1.0	1.5	2.0	5.0	10
Present	1.7107	0.8889	0.5564	0.1421	0.0618
Ansari <i>et al.</i> (2015)	1.7094	0.8887	0.5564	0.1420	0.0617

subjected to uniform loading $q = 1 \text{ N/m}^2$. Normalized deflection is defined by

$$\bar{w} = w_{\text{max}} \frac{100E_m h^3}{qa^4}. \quad (27)$$

\bar{w} is plotted with respect to power function exponent n for three different plate theories. When $n = 1$, all material variation profiles are linear. The plate is metal-rich for $n > 1$, and ceramic-rich if $n < 1$. Mid-point deflection is found to be an increasing function of the exponent n . This is the expected result since for larger n the plate is metal-rich, and elastic modulus of the metallic component is much smaller than that of ceramic component. Deflection profiles found in accordance with Kirchhoff plate theory and third-order shear deformation theory are close to each other, whereas MPT overestimates the micro-plate deflection. Further results generated for static bending presented in Figs. 4 and 5 are calculated by considering TSDT.

Fig. 4 illustrates influence of the length scale parameter variation upon the static bending behavior. Normalized maximum plate deflection is plotted as a function of the exponent n for four different values of the length scale parameter ratio β . Note that when $\beta = 1$, all length scale parameters of the strain gradient theory are constant, while any value other than unity implies through-the-thickness variations for these parameters. Maximum micro-plate deflection \bar{w} decreases as the ratio β is varied from 1/2 to 4. Impact of β upon static bending behavior underlines the importance of inclusion of length scale parameter variations in the formulation of micro-scale structural problems. Fig. 5 depicts variations of the maximum

Table 3 Dominant modes and corresponding frequencies, $l = 15 \mu\text{m}$, $l/h = 0.4$, $a/h = 10$, $b/a = 1.0$, $n = 2.0$

$\beta=1/2$		$\beta=4.0$	
$\bar{\omega}$	Dominant Mode	$\bar{\omega}$	Dominant Mode
14,0703	Transverse w , mode 1	33,7745	Axial, mode 1
32,6332	Axial, mode 1	33,7745	Axial, mode 1
32,6332	Axial, mode 1	41,4124	Transverse w , mode 1
33,7162	Transverse w , mode 2	48,8784	Axial, mode 2
33,7162	Transverse w , mode 2	74,6516	Axial, mode 3
45,6546	Axial, mode 2	74,6516	Axial, mode 3
52,0493	Transverse w , mode 3	82,6270	Axial, mode 4
63,6646	Transverse w , mode 4	85,4552	Axial, mode 5
63,6646	Transverse w , mode 4	85,4552	Axial, mode 5
65,8387	Axial, mode 3	99,8940	Transverse w , mode 2

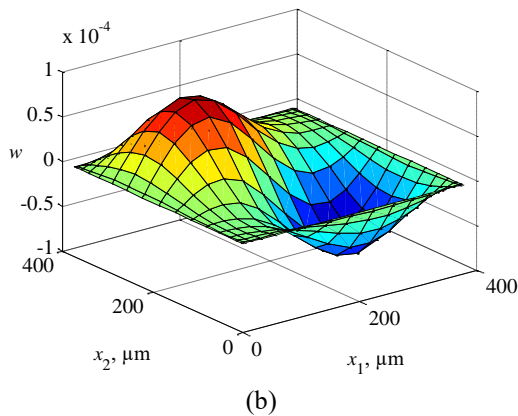
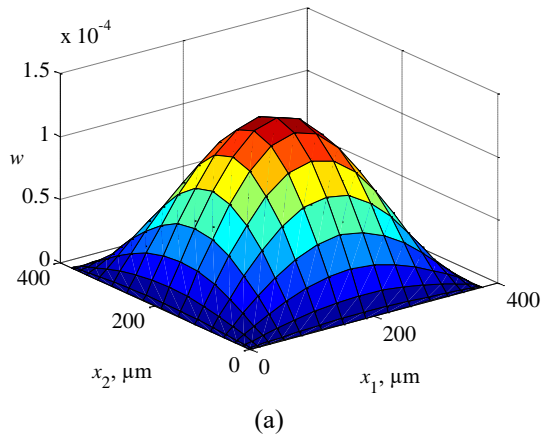


Fig. 7 Dominant transverse mode shapes: (a) Transverse mode 1 (w); (b) transverse mode 2 (w). $l = 15 \mu\text{m}$, $l/h = 0.4$, $a/h = 10$, $b/a = 1.0$, $n = 2.0$, $\beta = 2.0$

deflection with respect to the normalized length scale parameter l/h , where l is length scale parameter of the metallic component. The curves are plotted for four different values of the exponent n . Maximum normalized deflection decreases as l/h is increased from 0 to 1.2. Reduction in the deflection is due to size effect, which is more prominent when h is close to l . As l/h approaches

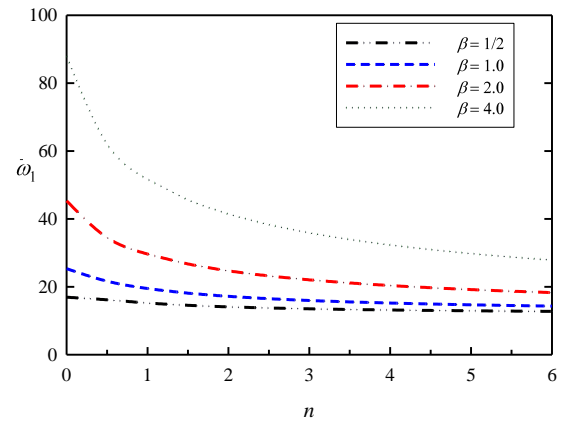


Fig. 8 First dimensionless transverse natural frequency $l = 15 \mu\text{m}$, $l/h = 0.4$, $a/h = 10$, $b/a = 1.0$

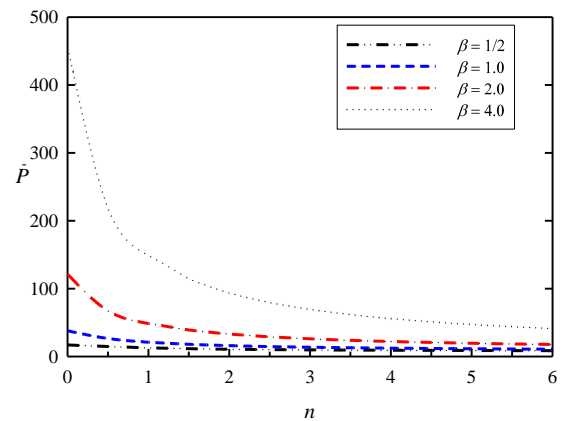


Fig. 9 Dimensionless critical buckling load, $l = 15 \mu\text{m}$, $l/h = 0.4$, $a/h = 10$, $b/a = 1.0$

zero, size effect weakens and this causes considerably larger deflections.

4.2 Free vibrations

In order to verify free vibration analysis techniques, in Table 2 we compare first natural frequencies of a simply-supported homogeneous micro-plate to the frequencies given by Ansari *et al.* (2015). Material properties are same as those given by Eq. (26), and MPT is used in analyses. Natural frequencies computed are found to be in excellent agreement.

Figs. 6-8 and Table 3 present our results regarding free vibrations of functionally graded rectangular micro-plates. Dimensionless natural frequency in this set of results is defined as

$$\bar{\omega} = \omega \frac{a^2}{h} \sqrt{\rho_m / E_m}. \tag{28}$$

Fig. 6 shows first dimensionless transverse natural frequency as a function of the exponent n for three different plate theories. Dimensionless frequency is found to be a decreasing function of n . Therefore, ceramic-rich micro-plates possess higher natural frequencies compared to

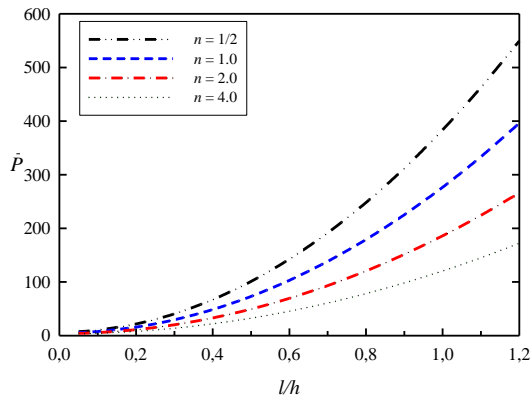


Fig. 10 Dimensionless critical buckling load, $h = 25 \mu\text{m}$, $a/h = 10$, $b/a = 1.0$, $\beta = 2.0$

metal-rich plates. Frequencies found in accordance with KPT and TSDT are in close agreement. MPT slightly underestimates the natural frequency. Remaining parametric analyses on free vibrations are thus carried out in accordance with TSDT.

Table 3 tabulates first ten dimensionless natural frequencies computed for length scale parameter ratios $\beta = 1/2$ and $\beta = 4$. The table also lists dominant mode of vibration at each frequency. The dominant mode is determined by comparing axial (u and v), transverse (w) and rotational (ϕ_1 and ϕ_2) mode shapes. Transverse vibration mode shapes of a simply-supported FGM micro-plate are illustrated in Fig. 7. The frequencies at which rotational vibration is dominant are generally the higher frequencies. Examining Table 3, it is seen that dominant mode of vibration strongly depends upon the length scale parameter ratio β . Fig. 8 depicts variation of the first dimensionless transverse natural frequency $\bar{\omega}_1$ with respect to n , for four different values of the length scale parameter ratio β . Increase in β causes a notable rise in the first dimensionless frequency. Thus, the micro-plate behaves in a stiffer manner for larger values of the length scale parameter ratio. Influence of β on vibration behavior is another finding illustrating the need to account for length scale parameter variation in structural analysis of micro-scale components.

4.3 Buckling

Numerical results regarding critical buckling loads of functionally graded rectangular micro-plates are provided in Figs. 9 and 10. For biaxial buckling, dimensionless critical buckling load is expressed in the form

$$\bar{P} = \frac{Pa^2}{E_m h^3}. \quad (29)$$

The results provided are generated by TSDT. Fig. 9 shows n -variation of the buckling load for four different values of the length scale parameter ratio β . Buckling load is highly sensitive to the changes in the length scale parameter ratio. It rises significantly as β is increased from $1/2$ to 4 . Fig. 10 presents variation of critical buckling load

with respect to l/h for four different values of n . This figure is illustrative of the size effect in that it shows that critical load computed for larger l/h is considerably larger than that evaluated for macro-scale plates for which l/h tends to zero.

5. Conclusions

In this article, we present new strain gradient elasticity-based analysis procedures for static bending, free vibrations, and buckling of functionally graded rectangular micro-plates. Proposed methods allow consideration of spatial variations of the length scale parameters. Analyses carried out in accordance with three different plate theories indicate that results found by Kirchhoff and third-order shear deformation theories are in very good agreement. Mindlin plate theory however slightly overestimates plate deflection, and underestimates free vibration frequency. Thus, third-order shear deformation theory could be used in micro-plate analysis because of higher-order variation of displacement field. Developed model allows assessment of micro-plate behavior for different types of FGM composition profiles. This is accomplished by changing the power function exponent n . It is numerically shown that ceramic-rich FGM micro-plates have lower static deflection and higher natural frequency compared to metal-rich plates. The figures displaying static deflection and buckling load as a function of l/h are illustrative of size effect. This effect becomes highly notable as l/h gets larger. Classical continuum theories are applicable at the other end of the spectrum, i.e. when l/h tends to zero. Length scale parameter ratio β identifies the degree of spatial variations of the length scale parameters. The ratio β is shown to have a significant impact on static deflection, vibration frequency, and buckling load of a rectangular FGM micro-plate. A rise in β leads to a drop in dimensionless maximum deflection, and increases in dimensionless vibration frequency and buckling load. Hence, sufficiently accurate results can be generated only if spatial variations of the length scale parameters are taken into account in the formulation of the relevant problem.

As part of future research activities, the developed procedures can be extended to examine mechanical behavior of micro-scale plates under different loading and environmental conditions. Thermal strains can be included in the formulation to analyze the response of micro-plates subjected to temperature gradients. Effect of time-dependent loads, such as harmonic, step, and impulsive forces, can be revealed by means of forced vibration analysis. Building the formulation of the problem on different non-classical theories such as modified couple stress theory, which employs a single length scale parameter; and nonlocal elasticity, which addresses nano-scale problems, could also be considered as an alternative venue for future work.

Acknowledgments

This work was supported by the Scientific and Technological Research Council of Turkey (TÜBİTAK)

through grant 213M606.

References

- Aghazadeh, R., Cigeroglu, E. and Dag, S. (2014), "Static and free vibration analyses of small-scale functionally graded beams possessing a variable length scale parameter using different beam theories", *Eur. J. Mech. A. Sol.*, **46**, 1-11.
- Aifantis, E.C. (1999), "Strain gradient interpretation of size effects", *J. Fract.*, **95**(1-4), 299-314.
- Akgöz, B. and Civalek, Ö. (2013), "Modeling and analysis of micro-sized plates resting on elastic medium using the modified couple stress theory", *Meccan.*, **48**(4), 863-873.
- Akgöz, B. and Civalek, Ö. (2015), "A microstructure-dependent sinusoidal plate model based on the strain gradient elasticity theory", *Acta Mech.*, **226**(7), 2277-2294.
- Alipour Ghassabi, A., Dag, S. and Cigeroglu, E. (2017), "Free vibration analysis of functionally graded rectangular nano-plates considering spatial variation of the nonlocal parameter", *Arch. Mech.*, **69**(2), 105-103.
- Andrew, W.M. and Jonathan, S.C. (2005), "Role of material microstructure in plate stiffness with relevance to microcantilever sensors", *J. Micromech. Microeng.*, **15**(5), 1060.
- Ansari, R., Faghih Shojaei, M., Mohammadi, V., Bazdid-Vahdati, M. and Rouhi, H. (2015), "Triangular mindlin microplate element", *Comput. Meth. Appl. Mech. Eng.*, **295**, 56-76.
- Ansari, R., Gholami, R., Faghih Shojaei, M., Mohammadi, V. and Darabi, M.A. (2013), "Thermal buckling analysis of a mindlin rectangular FGM microplate based on the strain gradient theory", *J. Therm. Stress.*, **36**(5), 446-465.
- Asghari, M. (2012), "Geometrically nonlinear micro-plate formulation based on the modified couple stress theory", *J. Eng. Sci.*, **51**, 292-309.
- Bellman, R.E. and Casti, J. (1971), "Differential quadrature and long-term integration", *J. Math. Anal. Appl.*, **34**, 235-238.
- Eringen, A.C. (1972), "Nonlocal polar elastic continua", *J. Eng. Sci.*, **10**(1), 1-16.
- Eshraghi, I., Dag, S. and Soltani, N. (2015), "Consideration of spatial variation of the length scale parameter in static and dynamic analyses of functionally graded annular and circular micro-plates", *Compos. Part B*, **78**, 338-348.
- Eshraghi, I., Dag, S. and Soltani, N. (2016), "Bending and free vibrations of functionally graded annular and circular micro-plates under thermal loading", *Compos. Struct.*, **137**, 196-207.
- Farahmand, H., Mohammadi, M., Iranmanesh, A. and Naserlavi, S.S. (2015), "Exact solution for free vibration analysis of functionally graded microplates based on the strain gradient theory", *J. Multisc. Comput. Eng.*, **13**(6), 463-474.
- Farokhi, H. and Ghayesh, M.H. (2015), "Nonlinear dynamical behaviour of geometrically imperfect microplates based on modified couple stress theory", *J. Mech. Sci.*, **90**, 133-144.
- Farokhi, H. and Ghayesh, M.H. (2016), "Nonlinear size-dependent dynamics of an imperfect shear deformable microplate", *J. Sound Vibr.*, **361**, 226-242.
- Fu, Y., Du, H. and Zhang, S. (2003), "Functionally graded TiN/TiNi shape memory alloy films", *Mater. Lett.*, **57**(20), 2995-2999.
- Gholami, R. and Ansari, R. (2016), "A most general strain gradient plate formulation for size-dependent geometrically nonlinear free vibration analysis of functionally graded shear deformable rectangular microplates", *Nonlin. Dyn.*, **84**(4), 2403-2422.
- Gurtin, M.E., Weissmuller, J. and Larche, F. (1998), "The general theory of curved deformable interfaces in solids at equilibrium", *Philos. Mag. A*, **178**, 1093-1109.
- Hassanin, H. and Jiang, K. (2014), "Net shape manufacturing of ceramic micro parts with tailored graded layers", *J. Micromech. Microeng.*, **24**(1), 015018.
- Jomehzadeh, E., Noori, H.R. and Saidi, A.R. (2011), "The size-dependent vibration analysis of micro-plates based on a modified couple stress theory", *Phys. E*, **43**(4), 877-883.
- Kahrobaiyan, M.H., Rahaeifard, M., Tajalli, S.A. and Ahmadian, M.T. (2012), "A strain gradient functionally graded euler-bernoulli beam formulation", *J. Eng. Sci.*, **52**, 65-76.
- Ke, L.L., Wang, Y.S., Yang, J. and Kitipornchai, S. (2012), "Free vibration of size-dependent mindlin microplates based on the modified couple stress theory", *J. Sound Vibr.*, **331**(1), 94-106.
- Kim, J. and Reddy, J.N. (2013), "Analytical solutions for bending, vibration, and buckling of FGM plates using a couple stress-based third-order theory", *Compos. Struct.*, **103**, 86-98.
- Kim, J. and Reddy, J.N. (2015), "A general third-order theory of functionally graded plates with modified couple stress effect and the von Kármán nonlinearity: Theory and finite element analysis", *Acta Mech.*, **226**(9), 2973-2998.
- Lam, D.C.C., Yang, F., Chong, A.C.M., Wang, J. and Tong, P. (2003), "Experiments and theory in strain gradient elasticity", *J. Mech. Phys. Sol.*, **51**(8), 1477-1508.
- Lazopoulos, K.A. (2009), "On bending of strain gradient elastic micro-plates", *Mech. Res. Commun.*, **36**(7), 777-783.
- Lou, J. and He, L. (2015), "Closed-form solutions for nonlinear bending and free vibration of functionally graded microplates based on the modified couple stress theory", *Compos. Struct.*, **131**, 810-820.
- Ma, H.M., Gao, X.L. and Reddy, J.N. (2011), "A non-classical Mindlin plate model based on a modified couple stress theory", *Acta Mech.*, **220**(1-4), 217-235.
- Mahmoud, F.F. and Shaat, M. (2015), "A new Mindlin FG plate model incorporating microstructure and surface energy effects", *Struct. Eng. Mech.*, **53**(1), 105-130.
- Mindlin, R.D. (1963), "Influence of couple-stresses on stress concentrations", *Exp. Mech.*, **3**(1), 1-7.
- Mindlin, R.D. (1965), "Second gradient of strain and surface-tension in linear elasticity", *J. Sol. Struct.*, **1**(4), 417-438.
- Mindlin, R.D. and Tiersten, H.F. (1962), "Effects of couple-stresses in linear elasticity", *Arch. Rat. Mech. Anal.*, **11**(1), 415-448.
- Mohammadimehr, M., Rousta Navi, B. and Ghorbanpour Arani, A. (2016), "Modified strain gradient reddy rectangular plate model for biaxial buckling and bending analysis of double-coupled piezoelectric polymeric nanocomposite reinforced by FG-SWNT", *Compos. Part B*, **87**, 132-148.
- Ng, C.H.W., Zhao, Y.B., Xiang, Y. and Wei, G.W. (2009), "On the accuracy and stability of a variety of differential quadrature formulations for the vibration analysis of beams", *J. Eng. Appl. Sci.*, **1**, 1-25.
- Nikolov, S., Han, C.S. and Raabe, D. (2007), "On the origin of size effects in small-strain elasticity of solid polymers", *J. Sol. Struct.*, **44**(5), 1582-1592.
- Park, S.K. and Gao, X.L. (2006), "Bernoulli-euler beam model based on a modified couple stress theory", *J. Micromech. Microeng.*, **16**(11), 2355.
- Ramezani, S. (2012), "A shear deformation micro-plate model based on the most general form of strain gradient elasticity", *J. Mech. Sci.*, **57**(1), 34-42.
- Reddy, J.N. and Kim, J. (2012), "A nonlinear modified couple stress-based third-order theory of functionally graded plates", *Compos. Struct.*, **94**(3), 1128-1143.
- Sahmani, S. and Ansari, R. (2013), "On the free vibration response of functionally graded higher-order shear deformable microplates based on the strain gradient elasticity theory", *Compos. Struct.*, **95**, 430-442.
- Salehipour, H., Nahvi, H. and Shahidi, A.R. (2015), "Exact closed-form free vibration analysis for functionally graded micro/nano

- plates based on modified couple stress and three-dimensional elasticity theories”, *Compos. Struct.*, **124**, 283-291.
- Setoodeh, A. and Rezaei, M. (2017), “Large amplitude free vibration analysis of functionally graded nano/micro beams on nonlinear elastic foundation”, *Struct. Eng. Mech.*, **61**(2), 209-220.
- Shenas, A.G. and Malekzadeh, P. (2016), “Free vibration of functionally graded quadrilateral microplates in thermal environment”, *Thin Wall. Struct.*, **106**, 294-315.
- Shu, C. (2000), *Differential Quadrature and its Application in Engineering*, Springer, London, U.K.
- Şimşek, M., Aydın, M., Yurtcu, H.H. and Reddy, J.N. (2015), “Size-dependent vibration of a microplate under the action of a moving load based on the modified couple stress theory”, *Acta Mech.*, **226**(11), 3807-3822.
- Stölken, J.S. and Evans, A.G. (1998), “A microbend test method for measuring the plasticity length scale”, *Acta Mater.*, **46**(14), 5109-5115.
- Thai, H.T. and Choi, D.H. (2013), “Size-dependent functionally graded kirchhoff and mindlin plate models based on a modified couple stress theory”, *Compos. Struct.*, **95**, 142-153.
- Thai, H.T. and Kim, S.E. (2013), “A size-dependent functionally graded Reddy plate model based on a modified couple stress theory”, *Compos. Part B*, **45**(1), 1636-1645.
- Thai, H.T. and Vo, T.P. (2013), “A size-dependent functionally graded sinusoidal plate model based on a modified couple stress theory”, *Compos. Struct.*, **96**, 376-383.
- Toupin, R.A. (1962), “Elastic materials with couple-stresses”, *Arch. Rat. Mech. Anal.*, **11**(1), 385-414.
- Tsiatas, G.C. (2009), “A new kirchhoff plate model based on a modified couple stress theory”, *J. Sol. Struct.*, **46**(13), 2757-2764.
- Wang, B., Zhou, S., Zhao, J. and Chen, X. (2011), “A size-dependent kirchhoff micro-plate model based on strain gradient elasticity theory”, *Eur. J. Mech. A. Sol.*, **30**(4), 517-524.
- Wang, Y.G., Lin, W.H. and Liu, N. (2013), “Large amplitude free vibration of size-dependent circular microplates based on the modified couple stress theory”, *J. Mech. Sci.*, **71**, 51-57.
- Witvrouw, A. and Mehta, A. (2005), “The use of functionally graded poly-SiGe layers for MEMS applications”, *Mater. Sci. For.*, **492-493**, 255-260.
- Yang, F., Chong, A.C.M., Lam, D.C.C. and Tong, P. (2002), “Couple stress based strain gradient theory for elasticity”, *J. Sol. Struct.*, **39**(10), 2731-2743.
- Yin, L., Qian, Q., Wang, L. and Xia, W. (2010), “Vibration analysis of microscale plates based on modified couple stress theory”, *Acta Mech. Sol. Sin.*, **23**(5), 386-393.
- Zhong, Z.Y., Zhang, W.M., Meng, G. and Wang, M.Y. (2015), “Thermoelastic damping in the size-dependent microplate resonators based on modified couple stress theory”, *J. Microelectr. Syst.*, **24**(2), 431-445.